31st International Conference Nuclear Energy for New Europe
NENE 2022 September 12-15 PORTOROŽ SLOVENIA

CFD Simulation of a VVER-1000/320 at Nominal Operating Conditions

Ossama Halim
Università di Pisa
Largo Lucio Lazzarino
56122, Pisa, Italy
ossama.abedelhalim@phd.unipi.it

Andrea Pucciarelli, Nicola Forgione
Università di Pisa
Largo Lucio Lazzarino
56122, Pisa, Italy
andrea.pucciarelli@unipi.it, nicola.forgione@unipi.it

ABSTRACT

A full-scale STAR-CCM+ model for VVER-1000/320 application purposes was developed in order to predict the core outlet temperature distribution, the pressure losses experienced at different locations and to investigate the mixing coefficients between loops, for in-vessel flow. The research activity was carried out in the framework of CAMIVVER project: "Code And Methods Improvements for VVER comprehensive safety assessment project". The primary aim of this work is to compare the measured and calculated core outlet temperature and mixing coefficient distributions at nominal operating conditions assessing the predicting capabilities of some selected turbulence models. The developed geometry consists of inlet nozzles, downcomer, lower plenum, core region, upper plenum, and outlet nozzles. The numerical simulations were performed using a computational grid of approximately 27.7 million polyhedral unstructured cells. The reference design of Kozloduy Unit 6 nuclear power plant was taken into account; with respect to the actual geometry of the vessel and its internals some simplifications were established in order to reduce the computational cost. Consequently, some regions were modelled as porous media, such as the core region, core basket, upper core plate, perforated barrel section and so forth. Also, additional pressure loss coefficients were imposed in the porous regions to reproduce the design pressure losses measured at the reference locations of Kozloduy-6 NPP. The CFD results predicted the presence of an azimuthal asymmetry of the loop flow centers relative to the cold leg axes, which is also observed in the experimental data. The azimuthal asymmetry shift is affected by the adopted turbulence model. Also, the distribution of the mixing coefficients at the fuel assemblies' outlet slightly differs based on the adopted turbulence model. The average values of the core outlet temperature distribution in the calculation are in the same range of the measured plant data. Overall, the results show a good agreement with the corresponding average plant measured parameters and provide a better understanding of the involved phenomena.

1 INTRODUCTION

The factors that influence the safe operation of pressurized water reactors (PWRs) are numerous and complex and include phenomena like mixing and turbulent flow. Computational fluid dynamics (CFD) is a well-suited tool to study such complex phenomena in detail. Since

there are large uncertainties in modelling the phenomena of interest, validation of CFD codes for reactor applications requires well-defined experiments.

B. Ivanov et al., 2002, conducted a coupled neutronic/thermal-hydraulic calculation and pointed out as the mixing that occurs in the VVER-1000 vessel is regarded as an unresolved issue in the analysis of complex plant transients with reactivity insertion [1]. Later, several studies were conducted to investigate the mixing phenomenon in detail using CFD models. U. Bieder et al., 2007, performed an LES analysis using the Trio-U CFD code for asymmetric flow distribution and found that Trio-U calculation correctly reproduced the measured rotation of the flow [2]. Moreover, T. Höhne et al., 2009, performed a comparison of three advanced CFD turbulence models considering the flow domain as the inlets nozzles, downcomer, lower plenum, and a part of the core, where all the turbulence models showed a consistent result corresponding to the measured values [3]. Also, M. Böttcher et al., 2010, compared a detailed model of a VVER-1000 reactor pressure vessel (RPV) and an extended model with simplified primary loops, where the RPV model predicted well the mixing in the RPV model, but the rotation of mixing patterns observed at the core inlet were not correctly reproduced and the loop model was limited by the computational time [4].

In the framework of the Codes And Methods Improvements for VVER comprehensive safety assessment project (CAMIVVER), a full scale three-dimensional CFD model is developed, in this work, for an improved description of the coolant mixing phenomena within the VVER RPV. The standard design of the VVER-1000 model V320 is considered; the reference data are derived from the operational data of the Kozloduy Unit 6 nuclear power plant (NPP) provided in the technical report [5]. A simplified full-scale model based on the porous media is developed and validated against Kozloduy-6 NPP designed plant data at nominal full power operating conditions, which serve as a preliminary step before being used for the VVER-1000 coolant transient benchmark.

2 GEOMETRY AND NUMERICAL MODEL SIMPLIFICATIONS

2.1 Geometry and Flow Characteristics

The VVER-1000/V320 is a pressurized water reactor of 3000 MW thermal power with four primary loops which produces 1000 MW of electric power. The nominal operating conditions of full power are 15.75 MPa of system pressure, 560.15 K of core inlet temperature and 17611 kg/s of reactor coolant mass flow rate. The Reactor Pressure Vessel (RPV) has four inlets and outlets nozzles to connect the primary loops and the primary sides of horizontal steam generators, as illustrated in the cross-sectional view of *Figure 1 (b)*. The core is comprised of 163 hexagonal fuel assemblies (FAs) without a shroud (i.e., open type core); each FA contains 312 fuel pins, where the total active core height is 3550 mm starting at 355 mm above the bottom of the FA.

The primary coolant enters from the inlet nozzles and mainly flows towards the downcomer; about 1% of the flow, instead, bypasses the core and directly reaches the hot leg through a spacer ring. After the downcomer, the flow reaches the elliptical bottom of the RPV, and it enters the perforated elliptical bottom of the core barrel which serves as distributor plate (see *Figure 1 (a)* bottom). As soon as the coolant passes through the perforated elliptical bottom of the barrel, part of the coolant flows upward through the fuel supporting columns and into the bottom of FAs and the other part enters the lower plenum through the perforated support columns. The heads of the FAs connect the core flow to the upper plenum, where the flow exits

to the outlet nozzles passing through the perforated frame of the shielding tubes block (see *Figure 1 (a)* top) and then through the perforated section in the barrel.

2.2 Numerical Model Simplifications and Meshing Properties

Due to the complexity of the RPV flow path, and in order to simulate the targeted mixing phenomena, a full 3D geometry of the VVER-1000 is developed considering several geometrical simplifications to fit the computational capabilities and reduce the computational cost. The simplifications for the RPV internal structures are listed as follows and the simplified model is shown in *Figure 1 (c)*:

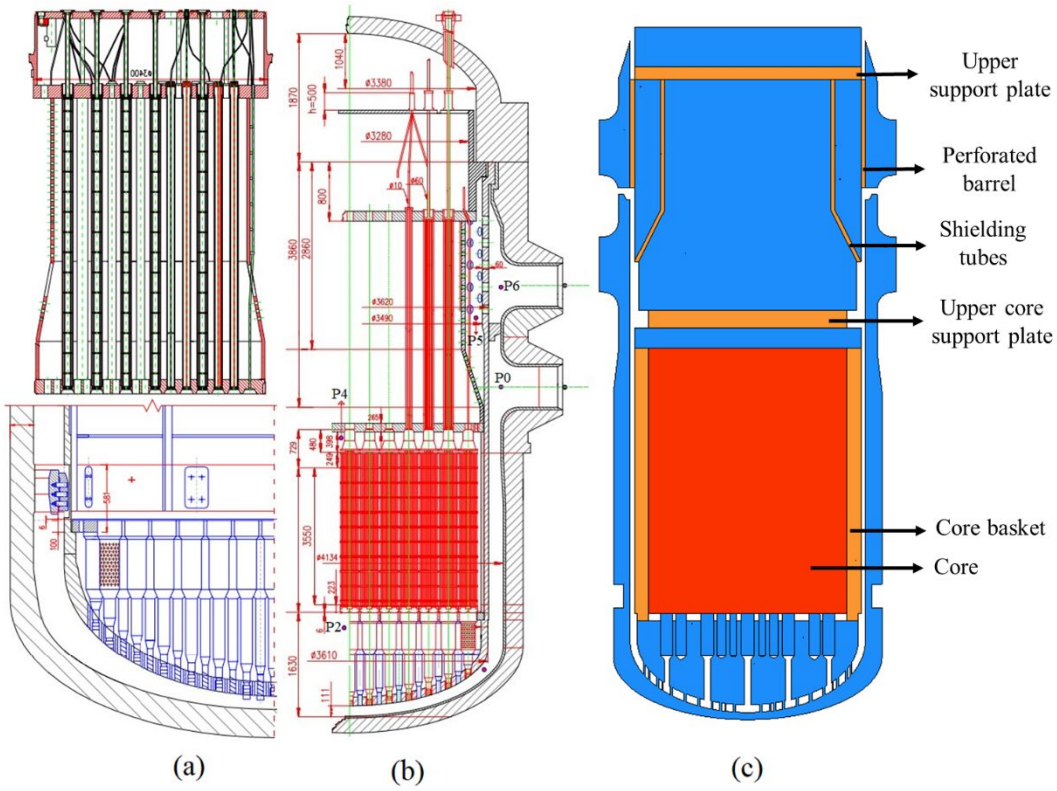

Figure 1. Sketch of (a) VVER lower plenum (bottom), upper plenum (top), (b) RPV, and (c) Cross sectional view of the modelled VVER vessel.

1) Only fluid regions are modelled; some internal structures and solid parts are modelled as porous media.
2) The flow bypass from the cold-leg to hot-leg is neglected and consequently the total mass flow at the inlets is reduced by 1% to compensate for the cold-hot legs bypass.
3) The core basket water cooling channels are modelled as a whole part connected to the lower plenum with the porous media treatment, to match the 3% core flow bypass corresponding to the actual plant data.
4) The perforated parts of the support columns are modelled as porous media interfaces.
5) The internal structures of FAs are not modelled explicitly; in fact, no fuel rods, control and instrumentation rods and water channels are modelled. The core region is instead modelled as 163 whole hexagonal FAs adopting again the porous media treatment.
6) The upper plenum internal structures are neglected, and the upper plenum zone is modelled as a fluid region, while the internal effects of the structures on the mixing phenomenon are considered to be negligible.

7) The perforated shielding tube block is modelled as a porous media region to reproduce the plant pressure losses between the exit of the FAs and right before the perforated section of the barrel.
8) The perforated section of the barrel is modelled as a porous media region to set the plant pressure losses between the exit nozzles and the inside barrel.
9) The two connection nozzles for the pressure safety injection system are neglected.

As a result of the geometrical simplifications mentioned earlier, the modelled domain consists of the 7 regions shown in *Figure 1 (c)*. Six porous regions are modelled due to the simplifications ahead prescribed; in which they are labelled in red (i.e., core) and orange (i.e., core basket, upper core support plate, shielding tube shroud, perforated section of the barrel and the upper plate) colours on *Figure 1 (c)*, while the blue colour represents a single region modelled as fluid. Thanks to the introduction of these porous media, the heat transfer processes between solid and fluid can be taken into consideration via the thermal non-equilibrium model, as well as reproducing the plant pressure losses through setting the porous resistance parameters not only in the stream wise direction but also in the radial and circumferential direction. All the considered assumptions contributed to reduce the total mesh element count and consequently reduce the computational time.

The computational grid of the fluid region is constructed by 24.8 million unstructured polyhedral cells, where 10 prism layers are used to resolve the near wall flow with a stretching factor of 1.5 and a total thickness of 25 mm. The core region contains approximately one million cells, constructed from 50 prismatic cell layers generated from polygonal cells. Eventually, all the porous regions are generated using unstructured polyhedral cells and constructed by 1.8 million cells. Therefore, the full geometry is constructed by a mesh grid of roughly 27.6 million cells; the size of the cells in the computational grid ranges from 20 mm up to 100 mm. It is important to notice that, since neither the fuel pins in the FAs nor the internal structure of the upper plenum is considered in the CAD, additional pressure losses are introduced in the porous regions to reproduce the design pressure losses measured at the positions P0, P2, P4, P5 and P6 as indicated on *Figure 1 (b)*, while operating at nominal conditions.

2.3 Numerical Model and Boundary Conditions

The STAR-CCM+ version 16.0 code was used to model the transport phenomenon of the fluid flow and heat transfer processes in the RPV. The thermophysical properties (density, dynamic viscosity, specific heat capacity and conductivity) of the coolant were introduced as temperature-dependent polynomials at a pressure of 15.5 MPa based on NIST REFPROP-V10 database [6]. The axial and radial power distribution maps were adopted to impose the internal heat source according to the technical report of A. Stefanova et al. [5]. The inlet boundary condition was set to be a uniform mass flow and the outlet boundary condition was set to be pressure outlet. The static temperatures were imposed at both inlets and outlets according to the plant data. The inlet turbulent settings were: 1% turbulent intensity and 10 viscosity ratio. The boundaries of the flow domain were modelled as adiabatic walls with no-slip conditions.

2.4 Turbulence Model

Several two-equation based turbulence models were considered to study their effects on the mixing phenomenon, such as the standard low-Reynolds k-ε (Lien et al., 1996) [7], k-ω Shear Stress Transport (SST) (Menter et al., 1994) [8] and elliptic blending k-ε models (Billard

et al., 2012) [9]. Second order convection discretization schemes were used for all transport equations, for all the RANS models adopted in this work. The all y+ wall treatment was used for near wall flow modelling. The heat transfer processes between solid and fluid in porous regions were modelled via the thermal non-equilibrium model and the solid properties set to be constant at the average temperature of the plant data [5]. Passive tracers were injected into the inlets to quantify the flow mixing at the core exit, as well as the azimuthal shift which occurs in the vessel.

3 RESULTS AND DISCUSSIONS

The RANS computations were carried out on a cluster of 2 processors, with total 56 cores and the simulation took approximatly 24 hrs to reach convergence. A set of thermo-dynamic parameters used to validate the turbulence models prediction, the pressure losses at the reference locations in the computational domain, the core inlet mass flow rate, core outlet temperature distribution and the mixing coefficient distribution at the core outlet were considered.

Table 1. shows a comparison of the plant pressure losses and the CFD predictions. The overall deviation from the plant data is not more than 2% and falls within the measurement error which is ± 0.043MPa [1]. Most pressure losses result from the P0-P2 section and the core region itself. All the turbulence models predicted the pressure difference across the core with a deviation of less than 1%, which reflects the adoption of suitable settings for the porous parameters in the core region. In addition, the pressure losses in the P4-P5 and P4-P6 are well predicted with respect to the plant data; this not only indicate the adoption of the suitable settings for the porous parameters, but also support the capability of using the porous media as an established numerical method to simplify complex flow geometries.

Table 1. Design pressure drops in the nominal steady state.

Location	Data (MPa)	EB k-e	k-ω SST	Standard k-e
P0-P2 from RPV inlet to the core inlet	0.1971	0.1989	0.1996	0.2002
P2-P4 in the core	0.1422	0.1419	0.1420	0.1420
P4-P5 outside the block of shielding tubes	0.0284	0.0290	0.0289	0.0290
P4-P6 in the upper plenum	0.0363	0.0370	0.0369	0.0370
P0-P6 in the reactor	0.376	0.3678	0.3675	0.3672

The CFD predictions for the rise of the core coolant temperature is approximately 33 K for all the three investigated turbulence models, the average core outlet temperature is lower than the designed value by 0.8 K. The core arrangement of the assemblies is illasturated in *Figure 2 (right)*; on the other hand, *Figure 2 (left)* shows a quantitative comparison of core outlet temperature distribution per assembly for the different turbulence models. As the higher temperature spikes per assembly can be attributed to the adopted radial power distribution map where the higher enrichment assemblies are located and the differences for all the three turbulence models are minors.

The average mass flow rate per assembly is 103.7 kg/s and the investigated turbulence models provide overall the same distribution at both core inlet/outlet. Though, some differences have been observed for the predicted mass flow at the center and the periphery of the core, especially at the inlet. *Figure 3*. shows a quantitative comparison of the core inlet/outlet mass flow distributions per assembly, where the maximum inlet mass flow rate is located at the periphery of the core, and the minimum inlet mass flow rate is located at the center. All the

turbulence models considered can resolve the symmetrical mass flow distribution around the axis of the RPV, thus demonstrating the reliability of the adopted simplified model.

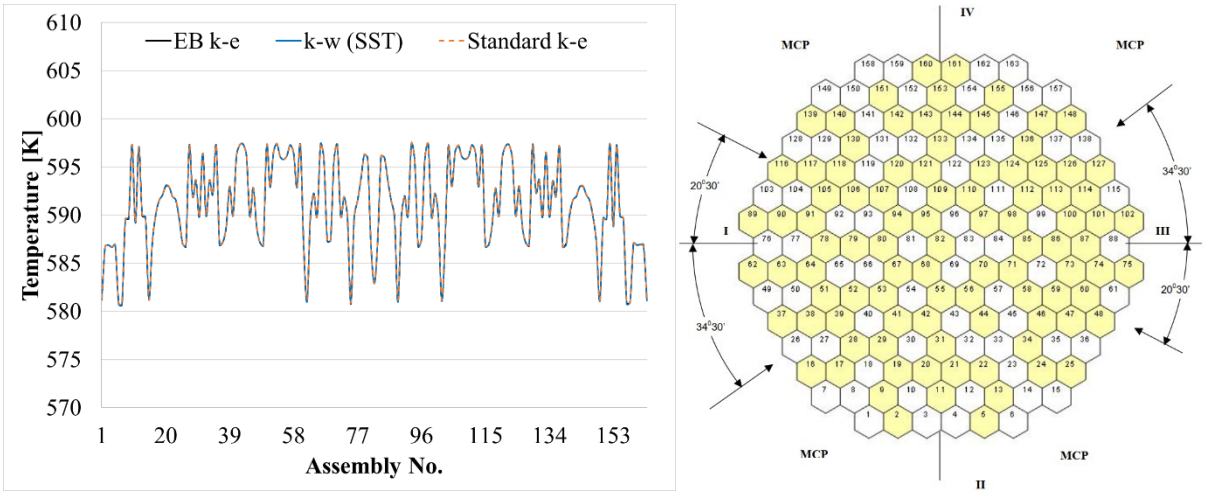

Figure 2. Core outlet temperature distribution (left), Core arrangement of the assemblies (right).

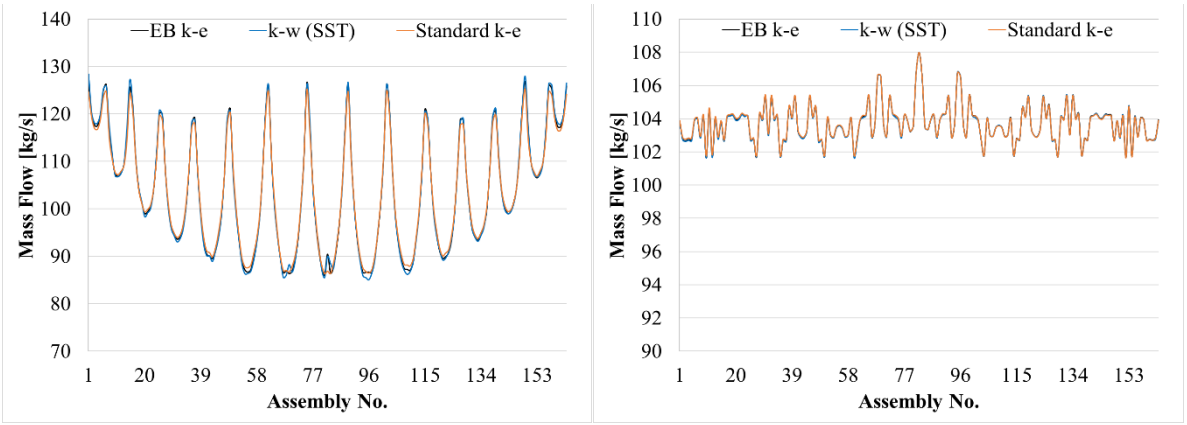

Figure 3. Assembly by Assembly core inlet (left)/outlet (right) mass flow distribution.

The mixing coefficients and the rotation for the flow center with respect to the inlet axis have been quantified to understand the effect of the adopted turbulence models on these quantities before being deployed to the VVER-1000 coolant transient benchmark. *Figure 4.* shows a quantitative core outlet mixing coefficient distribution for loops one and three, which are located opposite to each other's, compared to the mixing coefficients data from the plant. Though the experimental mixing coefficients were obtained at different boundary conditions at the steady state before the beginning of the coolant transient benchmark, the comparison was made for qualitative purposes to understand the role of the turbulence models on the investigated quantity, as it was based on the comparable values of the mass flow rates between the nominal steady state and the steady state before the beginning of the transient.

Actually, the mixing coefficients were estimated using a passive transported scalar, working as a tracer. As it is shown in *Figure 4*, all models provide a comparable overall trend with some discrepancies, starting with the highest concentrations for the passive tracer in the vicinity of the corresponding inlet and then gradually decreasing moving away from it. Although the overall trend of the mixing coefficient is similar, the size and the shape of the

non-mixing zone (i.e., assemblies having 90% and more flow from certain loop) of the passive tracer is dependent on the adopted turbulence model. *Figure 5.* shows a comparison of the core outlet mixing coefficients distribution for loop 1. While all the three turbulence models resolved the flow rotation for loop 1 to be counter-clockwise, the displacements are not the same, because it is computed as a function of the center of the non-mixing zone. *Table 2* shows the azimuthal shift of the loop flow centers, where all the adopted turbulence models predicted a degree of symmetry for the flow rotation of the opposite loops. Nevertheless, the values of the azimuthal shift of the loop flow centers infer that the SST k-ω model shows the lowest deviation among the other models which makes it a suitable candidate to be deployed in the VVER-1000 coolant transient benchmark.

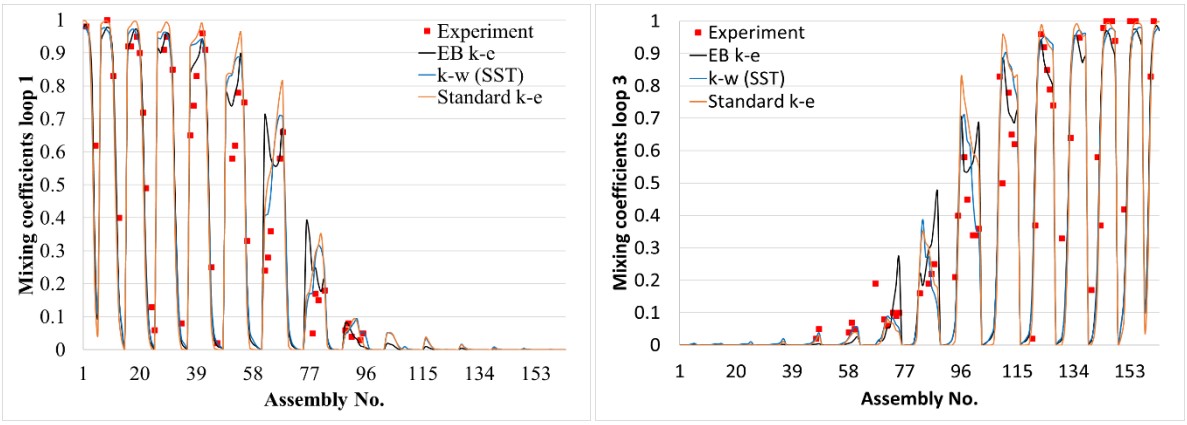

Figure 4. Assembly by Assembly core outlet mixing coefficients distribution.

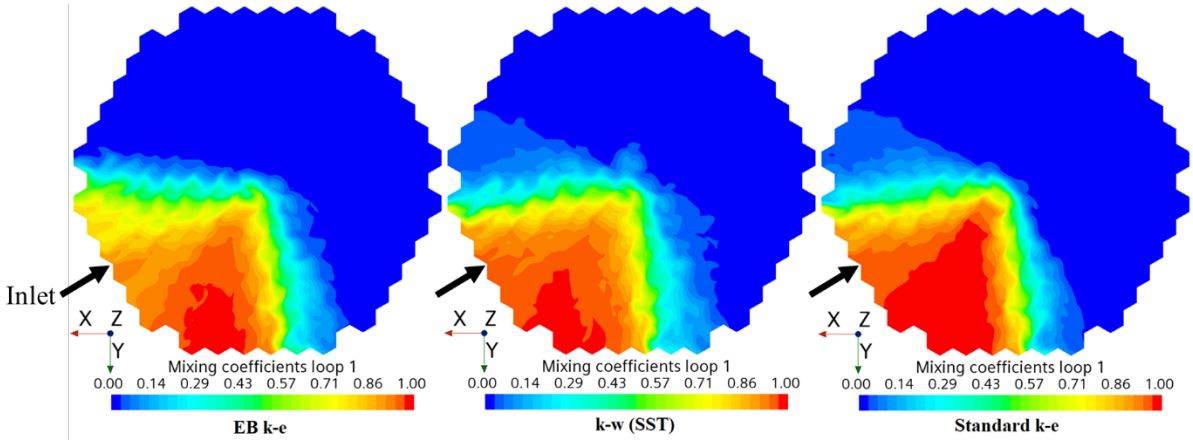

Figure 5. Core outlet mixing coefficients distribution for loop 1.

Table 2. Azimuthal shift of the loop flow centers.

	Unit 6 [◦]	EB k-e [◦]	k-ω SST [◦]	Standard k-e [◦]
loop 1	-24	-29.57	-22.09	-22.88
loop 2	8	15.38	11.81	16.24
loop 3	-30	-33.04	-21.84	-23.52
loop 4	8	13.25	12.01	17.11

4 CONCLUSIONS

A full-scale three-dimensional model has been developed, in order to predict not only the mass flow, temperature and pressure distributions, but also the mixing and flow rotation occurring in the RPV of a VVER-1000/320 at nominal operating conditions. A simplified

geometry was considered in several regions through the use of a porous media model with an appropriate porosity and resistance coefficient. The adopted simplifications allowed to reduce the total number of mesh counts and consequently the computational time. Though the use of simplified geometry was considered, the RPV characteristic parameters were predicted sufficiently well within the range of the plant measurement accuracy.

A validation of the obtained pressure losses across the RPV was performed by comparing the CFD predictions to Kozloduy-6 NPP data. The comparison showed a maximum deviation of 2% with respect to the plant data. The adopted turbulence models showed an overall similar trend for the mass flow and core outlet temperature distributions. The calculation showed the overall trend of the mixing coefficient is similar for all the adopted turbulence models, however, the flow rotation of the loop flow center is dependent on the turbulence model. The k-ω (SST) model showed a better degree of symmetry for the flow rotation of the opposite loops.

In the light of the obtained results, it can be confirmed that the simplified developed model for simulating flow and heat transfer characteristics in the RPV of the VVER-1000 under nominal steady state operating conditions is adequate and acceptable. The promising results obtained in the frame of the present work represent a valuable benchmark showing the capabilities of the adopted numerical approach; the reliability of the adopted model will be thus further assessed against transient operating conditions in the frame of future applications to be included in the CAMIVVER project.

ACKNOWLEDGMENTS

The Authors would like to thank the benchmark partners for their support and discussions, and especially FRAMATOME for providing the CAD file for this project. The work reported in this paper was carried out in the framework of the Codes And Methods Improvements for VVER comprehensive safety assessment project (CAMIVVER) as a part of H2020 CAMIVVER within project no. 945081.

REFERENCES

[1] Ivanov, Boyan, Kostadin Ivanov, Pavlin Groudev, Malinka Pavlova, and Vasil Hadjiev. "VVER-1000 coolant transient benchmark." NEA/NSC/Doc 6 (2002).

[2] Bieder, Ulrich, Gauthier Fauchet, Sylvie Bétin, Nikola Kolev, and Dimitar Popov. "Simulation of mixing effects in a VVER-1000 reactor." Nuclear Engineering and Design 237, no. 15-17 (2007): 1718-1728.

[3] Höhne, Thomas. "CFD Simula1tion of thermal-hydraulic benchmark V1000CT-2 using ANSYS CFX." Science and Technology of Nuclear Installations 2009 (2009).

[4] Böttcher, Michael, and Regina Krüßmann. "Primary loop study of a VVER-1000 reactor with special focus on coolant mixing." Nuclear Engineering and Design 240, no. 9 (2010): 2244-2253.

[5] Antoaneta Stefanova, Neli Zaharieva, Petia Vryashkova, and Pavlin Groudev, “The CAMIVVER Definition report with specification for NPP with VVER 1000 reactor with respect to selected transients”.

[6] Lemmon, E. W., Ian H. Bell, M. L. Huber, and M. O. McLinden. "NIST Standard Reference Database 23: Reference Fluid Thermodynamic and Transport Properties-REFPROP, Version 10.0, National Institute of Standards and Technology." Standard Reference Data Program, Gaithersburg (2018).

[7] Lien, F.S., Chen, W.L., and Leschziner, M.A. 1996. “Low-Reynolds number eddy-viscosity modelling based on non-linear stress-strain/vorticity relations”, Proc. 3rd Symp. on Engineering Turbulence Modelling and Measurements, 27-29 May, Crete, Greece.

[8] Menter, F.R. 1994. “Two-equation eddy-viscosity turbulence modeling for engineering applications”, AIAA Journal, 32(8), pp. 1598-1605.

[9] Billard, F., and D. Laurence. "A robust k− ε− v2/k elliptic blending turbulence model applied to near-wall, separated and buoyant flows." International Journal of Heat and Fluid Flow 33, no. 1 (2012): 45-58.